COBEM 2023 27TH INTERNATIONAL CONGRESS OF MECHANICAL ENGENEERING

ABCM Brazilian Society of Mechanical Sciences and Engineering
27th ABCM International Congress of Mechanical Engineering
December 04-08, 2023, Florianópolis-SC, Brazil

APPLICATION OF MICROWAVE HYBRID HEATING FOR PACK CHROMIZING OF THE AISI M2 TOOL STEEL

Vitor Silveira Rolin
Luciana Takahashi
Post-Graduate Program in Mechanical Engineering, São Paulo State University (UNESP). Avenida Brasil Centro, 56, Ilha Solteira, CEP 15385-000, SP, Brazil.
vsrolin@unesp.br, luciana.takahashi@unesp.br

Juno Gallego
Department of Mechanical Engineering, São Paulo State University (UNESP). Avenida Brasil Centro, 56, Ilha Solteira, CEP 15385-000, SP, Brazil.
juno.gallego@unesp.br

Abstract. *Failures caused by wear and corrosion can greatly shorten the life of engineering tools and parts. A solution to reduce these failures is the strengthening of surfaces by thermochemical treatments, such as pack chromizing. That treatment demands high temperatures and a long processing time, causing a high energy and time cost. Modern metallurgical processing claims more efficient and sustainable heating techniques, becoming microwave heating an innovative and promising process. In the present work a domestic microwave oven, operated at 2.45 GHz and with nominal power of 1050 W, was applied for pack chromizing of the AISI M2 tool steel samples performed at 1000 ℃ for 1 hour. High temperatures were obtained by hybrid heating mechanism, where a thermal insulated silicon carbide ring acting as susceptor was able to transfer heat to the samples. Pack chromizing samples were prepared insert small pieces of AISI M2 steel (5 x 5 x 20mm) into a powder mixture composed by Cr-rich iron alloy acting as diffusion metal, ammonium chloride (NH_4Cl) as activator and aluminum oxide (Al_2O_3) as inert compound. Temperature was measured by K-type thermocouple. After air cooling samples were investigated by optical and scanning electron microscopy, EDS microanalysis, X-ray diffraction (XRD) and Vickers microhardness. The innovative treatment was able to form hard chromium-rich coatings on the surface of AISI M2 steel samples, which average thickness was 6.9 µm. Microstructure analysis have shown that coatings are composed by 2 distinctive layers, formed due to partition during diffusion of the chromium from mixture with the iron and carbon from the steel. XRD results show that outer layer is mainly composed by $Cr_2C_{0.46}N_{0.44}$ orthorhombic chromium carbonitride and few body-centered cubic ferrite. Vickers microhardness of the chomized surfaces has attained 1898 ± 156HV, near 3.7 times harder than substrate/matrix. The obtained results confirm that microwave hybrid heating is a faster e quite promising metallurgical process to improve surface properties for tool steels*

Keywords: *coating; pack chromizing; microwave hybrid heating.*

1. INTRODUCTION

Engineering components are subject to mechanical failures, the vast majority of which are caused by wear and corrosion. The application of a coating on the surface can change its properties, thus reducing degradation subject to wear and corrosion (SINGH et al., 2021). The chromizing process is one of the surface modification techniques that has been used for years, and one of its forms of application is pack chromizing (LEE and DUH, 2004). Fernandes et al., (2012) mention that pack chromizing is a technique considered effective, low-cost and enables the coating of parts with different geometries.

The pack chromizing process is a method where metal is placed in a box buried in a mixture of powdered chromium, activator compound and an inert compound. The process has two steps: in the first, the halide salt activator reacts with the chromium and forms gaseous halides that deposit on the metal. In the second, chromium diffuses to the metal surface (LEE and DUH, 2004).

In search of a more efficient, economical and clean heating technique, several authors have turned their attention to the use of microwaves for applications in metals, as recently demonstrated by studies such as Pechoto (2022) who used microwave irradiation to the foundry of non-ferrous metals, Sahota et al., (2021) and Singh et al., (2021) in their reviews demonstrate microwave applications for metal welding and surface treatments and Takahashi (2022) who applied a chromium coating on tool steel using hybrid microwave heating. Microwave heating occurs differently from heating by conventional techniques, Mishra and Sharma (2016) explain that microwaves transform electromagnetic

energy into heat, inside the material, leading to rapid and uniform heating. However, this heating depends on the properties of the material and the interaction with the magnetic field.

Materials can be classified according to their interaction with microwaves, Gupta (2007) describes that materials can be transparent, being those materials with low dielectric loss that do not absorb electromagnetic waves, allowing them to pass directly through the material. Absorbent materials are those with high dielectric loss, capable of absorbing microwave energy and converting it to heat efficiently. Opaque or reflective materials that have high electrical conductivity, such as metals and their alloys, whose microwave reflection at room temperature does not allow significant penetration to act on heating a massive material. Mishra and Sharma (2016) define that the depth of penetration is directly impacted by the conductivity of the material, so that materials with high conductivity have a lower depth of penetration.

The penetration depth of microwaves decreases as the conductivity of the material increases. Because they are excellent conductors, metals have a very small penetration depth, therefore, it is only possible to heat them directly in the form of a very fine powder. (LINGAPPA et al., 2017). For the heating of metals in massive quantities, there is a need to employ a hybrid microwave heating technique, using a susceptor (absorbing material), to start heating the metallic material until it reaches the critical temperature (BHATTACHARYA and BASAK, 2016). In his study Lingappa et al., (2017) suggests that metals begin to absorb microwaves when they reach approximately 50% of the melting temperature, which is called the critical temperature. The metal demonstrates linear heating until it reaches this temperature and after absorption of microwaves the rate of heating becomes exponential.

2. MATERIALS AND METHODS

Samples of square section with dimensions 5 x 5 x 20mm of an AISI M2 tool steel were coated using a pack chromizing technique. For the application of this technique a powder mixture composed of 35 wt% Cr-rich iron alloy acting as diffusion metal, 5 wt% ammonium chloride (NH_4Cl) as activator and 60 wt% aluminum oxide (Al_2O_3) as inert compound. The proportions used here were based on the study by Fernandes et al. (2012). The AISI M2 tool steel and its chemical composition were obtained from the GGD metals company and the Fe-Cr alloy with its composition were supplied by Cofel Comercial e Indústria de Ferro Ligas. The chemical compositions are showed in Table 1.

Table 1- Chemical composition in % mass of AISI M2 steel and Fe-Cr diffusion metal

	C	**Mn**	**Si**	**Cr**	**Mo**	**W**	**V**	**P**	**S**	**Fe**
AISI M2	0.9	0.3	0.3	4.2	5	6.2	1.9	-	-	81.2
Fe-Cr	0.05	-	0.34	71.00	-	-	-	0.02	0.02	28.57

The assembly of the system for hybrid heating of the samples is illustrated in the Figure 1. Three samples, named FeCr1, FeCr2 and FeCr3, were prepared. They were placed in the center of graphite tubes buried in the powder mixture, a graphite sheet was placed on the surface and later the tubes were closed and sealed with refractory cement. The tubes were placed in a graphite crucible and heated at 1000°C for 60 min using hybrid heating in a domestic microwave with a nominal power of 1050W and a frequency of 2.45GHz. Microwave hybrid heating was carried out using a silicon carbide (SiC) ring as a susceptor and an alumina-based ceramic fiber blanket acting as a thermal insulator. In the upper part of the crucible, a mixture of charcoal and sodium silicate was added, aiming to reduce the oxygen in the medium with the burning of coal. The temperature was monitored using a K-type chromel-alumel thermocouple, being recorded at intervals of 1 second by a datalogger-type temperature data recorder according to procedure detailed by Takahashi (2022).

After treatment and cooling in air, cross sections of the sample were cut and subjected to standard metallographic preparation. The formed layers were investigated by optical (OM) and scanning electron microscopy (SEM), microanalysis by energy dispersive electron spectroscopy (EDS), X-ray diffraction (XRD) and Vickers micro hardness. Image analysis was performed on the obtained digital images with help of the ImageJ software, while on the XRD patterns Rietveld refinements were applied with PROFEX software. Phase identification was based on crystallographic information files (CIF) available in the Inorganic Crystal Structure Database (ICSD). Analyses of Variance (ANOVA) were applied on the obtained results using 5% of significance level.

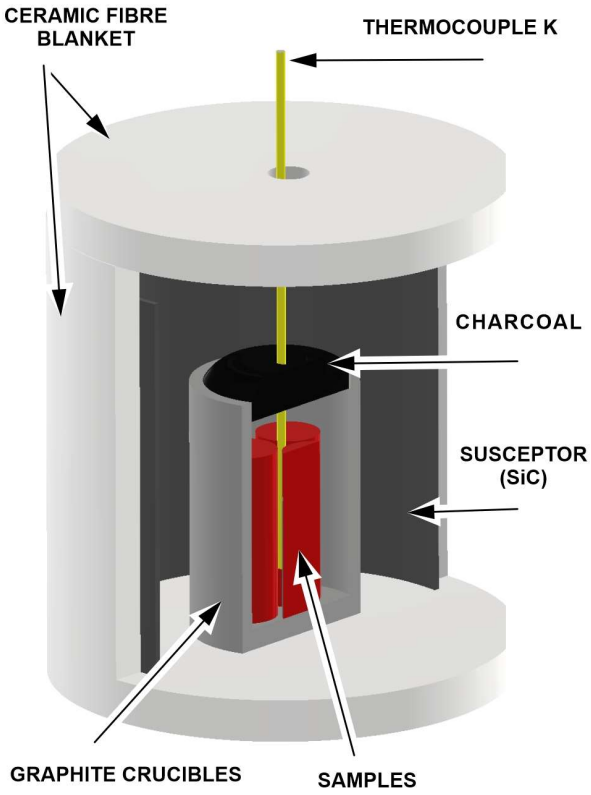

Figure 1- Schematic representation of the hybrid microwave heating system.

3. RESULTS AND DISCUSSIONS

The thickness of the chrome-rich coating formed on the surface of the tool steel was obtained using optical micrographs of the cross section of the samples and the free software ImageJ. The optical micrographs of FeCr1, FeCr2, and FeCr 3 samples are seen in Figure 2.

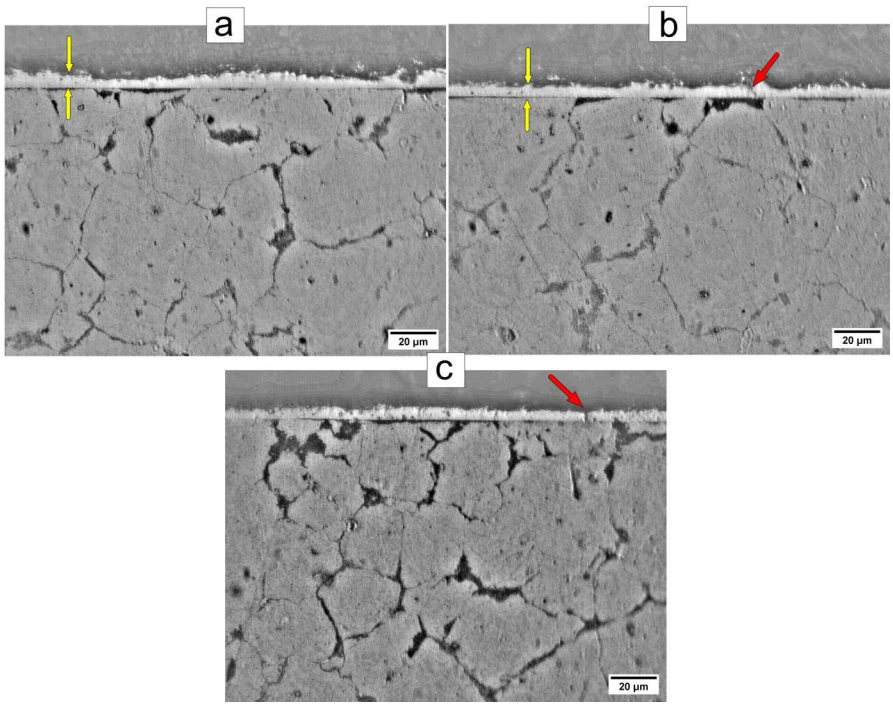

Figure 2- Optical micrographs of the cross section of the samples a) FeCr1, b) FeCr2 and c) FeCr3, after chromized for 1 hour at 1000°C.

Indicated by the yellow arrows, there is a continuous layer involving the entire perimeter of the cross section of the sample, however with the presence of some small cracks as indicated by the red arrows. Based on ASTM E-112, the grain sizes of substrates from FeCr1 and FeCr2 samples were measured, showing mean sizes of 24.9 ± 2.9 µm and 22.1 ± 1.8 µm, respectively. Thus, showing that the thermal cycle for both samples were similar, not impacting on a significant difference between grain sizes. The Figure 3 shows the variation in the thickness of the chrome-rich coating formed on the faces of the samples.

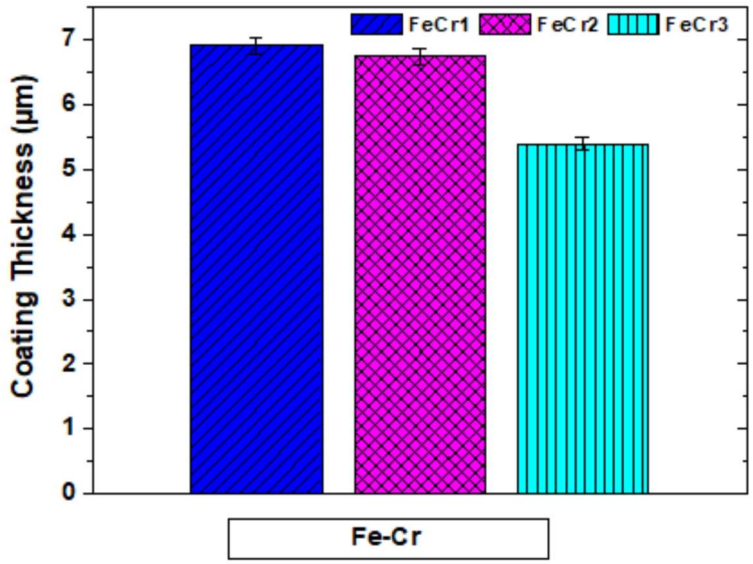

Figure 3- Layer thickness variations in samples after chromized for 1 hour at 1000°C.

The coating formed on the FeCr1 sample showed a thickness ranging from 5.7 ± 0.3 µm to 7.7 ± 0.5 µm, with a mean 6.9 ± 0.2 µm. Statistical analysis showed that there was significant variation in only 1 of the 4 faces. The FeCr2 sample shows a similar coating, having a thickness varying between faces from 6.1 ± 0.5 µm to 7.6 ± 0.6 µm and an average of 6.7 ± 0.2 µm. Statistical analysis again showed significant variation in only 1 of the 4 faces. The FeCr3 sample presented a coating with a thickness between the faces ranging from 4.9 ± 0.2 µm to 5.9 ± 0.3 µm and an average of 5.4 ± 0.2 µm, demonstrating the smallest thickness among the samples.

To observe finer features of microstructure the coatings were analyzed by Scanning Electron Microscopy (SEM), which typical aspect can be seen in Figure 4.

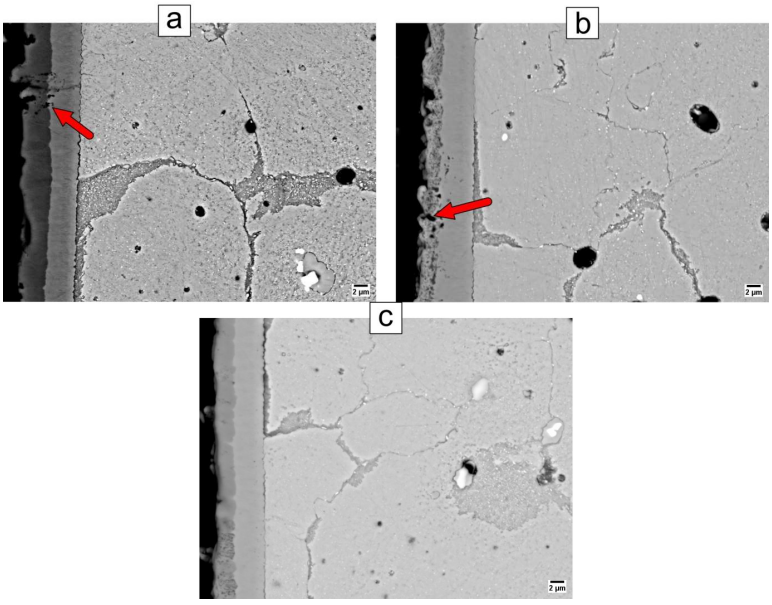

Figure 4 - Scanning electron micrograph of the cross-section of samples a) FeCr1, b) FeCr2 and c) FeCr3 after chromized for 1 hour at 1000°C.

In all samples, it was observed that the coating is composed of two regions of distinct morphology, an inner region of lighter tone with homogeneous thickness and no visible defects and a more irregular outer layer, with the presence of microcracks and microspores (indicated by the red arrows). The presence of microspores is presumably caused by the difference in the diffusion coefficients of the elements that diffused in the layer, indicating the occurrence of the Kirkendall effect (PAZ Y PUENTE and DUNAND, 2020), an effect already reported by several authors, including Lee et al., (2002) when applying a chromium coating on a two-phase Fe-Mn-Al-Cr alloy and also by Dong et al., (2019) who applied a chromium coating on a 316L stainless steel by pack chromizing.

The EDS mapping of the FeCr1 and FeCr2 samples was performed, the mapping of the elemental chemical composition is shown in Figure 5.

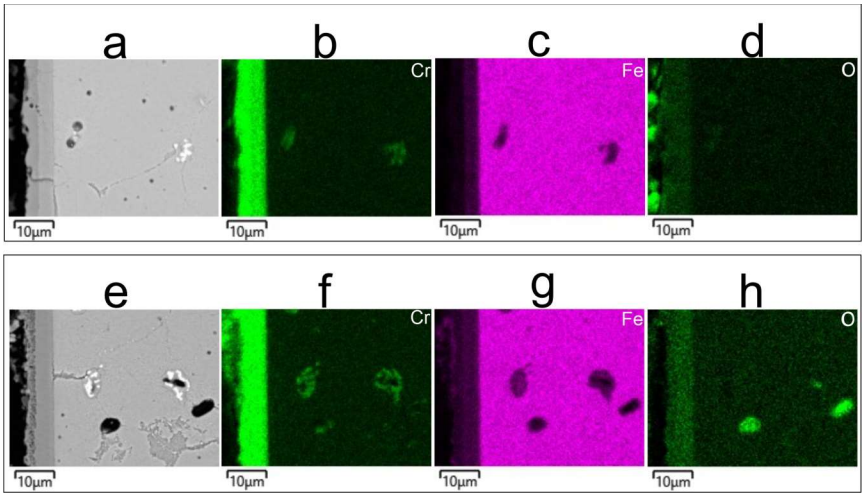

Figure 5- EDS mapping by chemical element of the cross section of FeCr1 sample (a,b,c and d) and FeCr2 sample (e,f,g and h).

Figures 5b and 5f show that the coating is mainly composed of Chromium, demonstrating a high concentration of this element in all regions of the layer with small concentrations in the substrate. The tool steel used has 4.2% by weight of Cr in its composition, explaining the distribution of this element in small quantities on the substrate. The layer has two distinct regions, with a higher concentration of Fe being observed in the inner layer close to the substrate in Figure 5c, demonstrating that Cr and Fe are solubilized together in this region. Figures 5d and 5h show the presence of Oxygen, with a higher concentration in the layer in relation to the substrate, suggesting the formation of oxides in this region. The large concentration of O observed in Figure 5.d is in a region external to the layer, this region being composed by Bakelite and Durofast – a reinforced ceramic compound responsible to the edge-retention of samples and a possible source for higher oxygen concentration.

SEM-EDS line scans of the FeCr1 and FeCr2 samples were performed, and the scan regions are shown in Figure 6.

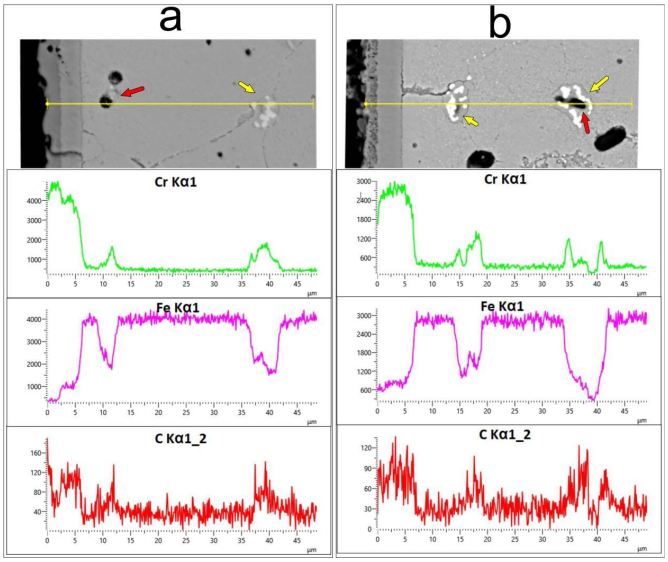

Figure 6- SEM-EDS line scan analysis of the cross section of the FeCr1 sample a) and FeCr2 sample b).

In the Figure 6 it is possible to see the peak of the Cr element in the coating, showing a sharp drop with the displacement of the line towards the substrate, the opposite is seen in the Fe element, with peaks in the substrate, decaying in the coating and in the black dots (red arrow) and white (yellow arrow). The element carbon is present in the coating, also presenting a peak in the black (red arrow) and white (yellow arrow) points, suggesting the presence of phases containing carbon in these regions.

To identify the phases present in the chrome-rich coating X-ray diffraction of the FeCr1 sample is shown in Figure 7. Similar XRD results were obtained to the other samples, FeCr2 and FeCr3, not presented here.

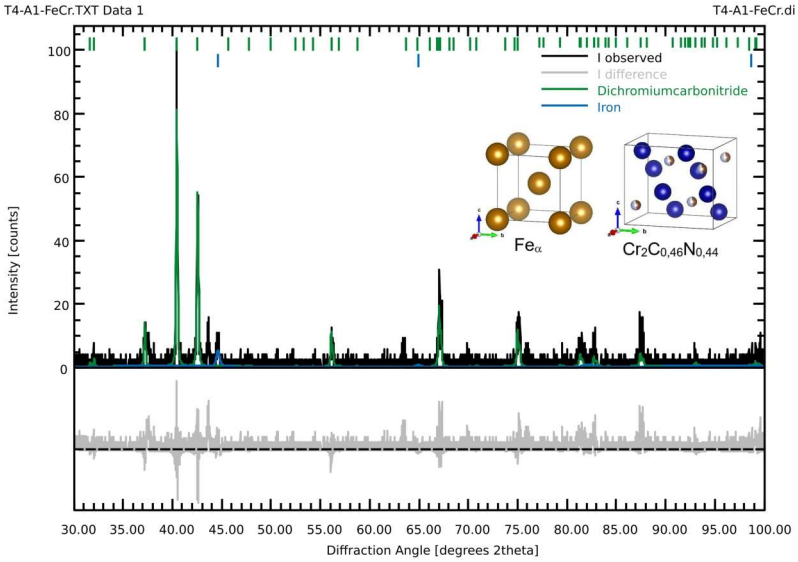

Figure 7- X-ray diffraction of the FeCr1 sample, with phases illustrated.

As demonstrated by the refracted peaks, the outer region of the coating is primarily formed by $Cr_2C_{0,46}N_{0,44}$ orthorhombic chromium carbonitrides (ICSD 31002), with a small concentration of body-centered cubic iron Feα (ICSD 52258). The Rietveld refinement with a goodness of fit (GOF) of 1.08 estimated the Feα concentration to be 4.9%, with the remainder being chromium carbonitrides. The results obtained are consistent with the literature, when compared with other authors such as Fernandes et al., (2012), Li et al., (2009) and Lee and Duh (2004), all reported in their studies the presence of the $(Cr,Fe)_2N_{1-x}$ phase in the coating. The formation of $Cr_2C_{0,46}N_{0,44}$ results from chemical reactions between the chromium from the FeCr alloy, the N from the decomposition of the NH_4Cl activator and the carbon from the substrate, like that portrayed by Lee and Duh (2004).

The samples were subjected to Vickers microhardness tests, measurements were made on the layer and on the substrate. The test data are presented in the graph of Figure 8.

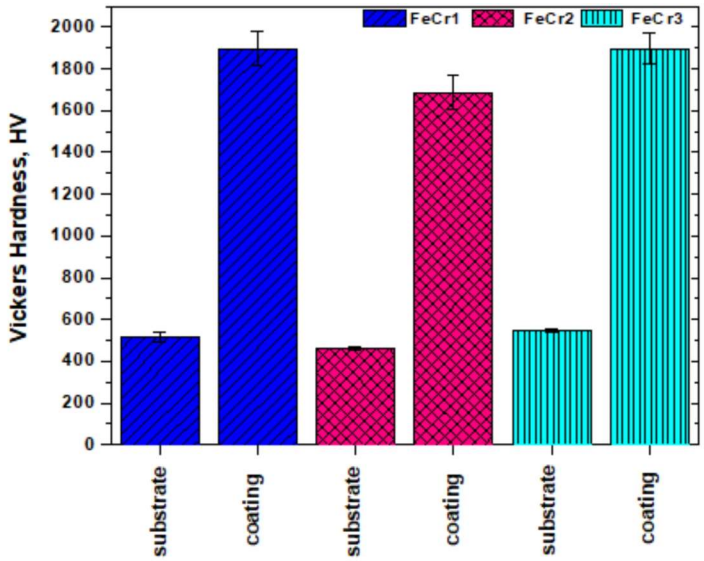

Figure 8- Variation of the Vickers microhardness of the samples after chromizing for 1 hour at 1000°C.

The coatings presented average hardness ranging from 1688 ± 164 HV to 1898 ± 156 HV, in relation to the values of 462 ± 17 HV to 550 ± 17 HV of the substrate, thus corresponding to an increase in hardness up to 3.7 times. The chrome coating applied with hybrid microwave heating showed hardness values like those of coatings conventionally made with an electric oven by Fernandes et al. (2012).

4. CONCLUSIONS

The powder mixture used with hybrid microwave heating has demonstrated to be effectiveness in forming a hard coating on the surface of the tool steel. The thickness of Cr-rich layer had varying from 5.7 to 7.7 μm, being mainly composed by chromium carbonitride with hardness of 1898 ± 156 HV, approximately 3.7 times harder than tool steel substrate.

5. ACKNOWLEDGEMENTS

The authors thank CAPES and CNPq for granting the scholarships and COFEL Comercial e Indústria de Ferro Ligas that kindly supplied Cr-Fe alloy applied in this work.

6. REFERENCES

AMERICAN SOCIETY FOR TESTING AND MATERIALS – ASTM. ASTM E112: Standard Test Methods for Determining Average Grain Size. West Conshohocken, 2013.

BHATTACHARYA, M.; BASAK, T. A review on the susceptor assisted microwave processing of materials. Energy, v. 97, p. 306-338, 2016.

DONG, Z.; ZHOU, T.; LIU, J.; ZHANG, X.; SHEN, B.; HU, W.; LIU, L. Effects of pack chromizing on the microstructure and anticorrosion properties of 316L stainless steel. Surface and Coatings Technology, p. 86-96, 2019.

FERNANDES, F. A. P.; HECK, S. C.; PICON, C. A.; TOTTEN, G. E.; CASTELETTI, L. C. Wear and corrosion resistance of pack chromised carbon steel. Surface Engineering, v. 28, n. 5, p. 313-317, 2012.

GUPTA, M.; LEONG, E. W. W. Microwaves and Metals. Singapure: John Wiley & Sons, 2007.

LEE, J.-W.; DUH, J.-G. Evaluation of microstructures and mechanical properties of chromized steels with different carbon contents. Surface and Coatings Technology, v. 177-178, p. 525-531, 2004.

LEE, J. W.; DUH, J. G.; TSAI, S. Y. Corrosion resistance and microstructural evaluation of the chromized coating process in a dual phase Fe–Mn–Al–Cr alloy. Surface and Coatings Technology, v. 153, p. 59-66, 2002.

LI, C. L.; LIN, Y. T.; LEE, J. W. Mechanical properties evaluation of chromized tungsten carbide–cobalt hardmetals. Surface & Coatings Technology, v. 204, p. 1106-1111, 2009.

LINGAPPA, S. M.; SRINATH, M. S.; AMARENDRA, H. J. An experimental investigation to find the critical (coupling) temperature in microwave hybrid heating of bulk metallic materials. Materials Research Express, v. 4, 2017.

MISHRA, R. R; SHARMA, A. K; A Review of Research Trends in Microwave Processing of Metal-Based Materials and Opportunities in Microwave Metal Casting. Critical Reviews in Solid State and Materials Sciences, V. 41, p. 217-255, 2016.

PAZ Y PUENTE, A. E.; DUNAND, D. C. Effect of Cr content on interdiffusion and Kirkendall pore formation during homogenization of pack-aluminized

PECHOTO, L. O; Fusão de metais não-ferrosos usando irradiação de micro-ondas. 2022. 66 f. Dissertação (Mestrado em Engenharia Mecânica) - Universidade Paulista “Júlio de Mesquita Filho”, Ilha Solteira, 2022.

SAHOTA, D. S; BANSAL, A; KUMAR, V. Application of microwave in welding of metallic materials – A review. Materials Today: Proceedings, V. 43, p. 466-470, 2021.

SINGH, P; GOYAL, D.P; BANSAL, A. Microwave heating: Fundamentals and application in surface modification of metallic materials – A review. Materials Today: Procedings. V. 43, p. 564-571, 2021.

TAKAHASHI, L; Cromização em caixa do aço ferramenta aisi m2 utilizando irradiação por micro-ondas como fonte de aquecimento. 2022. 95 f. Dissertação (Mestrado em Engenharia Mecânica) - Universidade Paulista “Júlio de Mesquita Filho”, Ilha Solteira, 2022.

7. RESPONSIBILITY NOTICE

The authors are solely responsible for the printed material included in this work.